Simple-Made-Continuous Steel Bridges With Steel Diaphragms

ROBERT I. JOHNSON and REBECCA A. ATADERO

ABSTRACT

Simple-made-continuous (SMC) bridges are a relatively new innovation in steel bridge design. The majority of SMC bridges currently in use are constructed with concrete diaphragms. This article presents the results of numerical analysis and physical laboratory testing of an alternative simple-made-continuous (SMC) connection scheme that uses steel diaphragms in lieu of concrete diaphragms. A bridge using steel diaphragms was constructed by the Colorado Department of Transportation in 2005, and the connections on this bridge serve as the basis for the research discussed herein. The results of the analysis and testing provided information for the development of a design methodology based on the physical behavior of the SMC connection. The paper also compares the steel-diaphragm SMC connection to concrete-diaphragm SMC connections and demonstrates that the steel-diaphragm design has several desirable features. For a diaphragm cost, which is similar in cost to other SMC schemes, the steel-diaphragm design requires less total construction time. Additionally, because the girder ends are exposed, it is easy to verify that the girders have fully weathered (for weathering steel), they may be easily inspected, and there is no concern about cracking of a concrete diaphragm at re-entrant corners around the steel bridge girders.

Keywords: steel bridges, composite steel girders, steel diaphragms, simple-made-continuous (SMC).

INTRODUCTION

Simple-made-continuous (SMC) bridges (also known as simple for dead–continuous for live, or SD-CL) are a relatively new innovation in steel bridge design. The majority of steel girder bridges using the SMC concept have steel girders cast into concrete-diaphragm beams on concrete piers, and a significant quantity of research has been performed on these types of SMC bridges (Azizinamini, 2014b). The subject of this article is an alternative SMC design using steel wide flange shape diaphragms and concrete support piers, which leave the entire steel structure exposed. A bridge of this type was constructed by the Colorado Department of Transportation (CDOT). It is shown prior to the placement of the concrete deck in Figure 1 and in its condition at the time of this writing in Figure 2. The specific detail was developed by CDOT due to depth limitations over an existing creek to be bridged. Originally, concrete bulb tees were considered; however, their depth did not provide the necessary 2-ft clearance over the high water level. The choice was made to use steel girders with SMC end connections (NSBA, 2006). At the time, the concept was commonly used with precast concrete beams, and CDOT felt that the same concept could be modified to be used with steel girders.

The connection is considered in the present research because the detail is straightforward, it allows the ends of the girders to be exposed to fully weather and to be visible for periodic inspection, and SMC bridges using steel diaphragms with exposed ends have not been the subject of previous research efforts. These bridges not only have the advantages of being simpler in design and faster to construct than conventional fully continuous bridges, but they are also more than 15% less in cost than fully continuous bridges. This paper describes physical testing and analysis of the steel-diaphragm SMC bridge connection and provides cost comparisons to other SMC schemes and fully continuous girder bridges.

BASICS OF SMC BEHAVIOR

As described in previous AISC *Engineering Journal* articles (Azizinamini, 2014a; Farimani, 2014), simple-made-continuous bridge girders in effect act as simple beams for the dead load of the bridge superstructure and act as continuous beams for live loads and superimposed dead loads. The behavior is achieved by placing simple span bridge girders, which are typically cambered for the precomposite dead loads (Figure 3). After the girders are installed, the slabs are formed and top and bottom bending and shrinkage reinforcing is placed for the slab along with additional top

Robert I. Johnson, Ph.D., S.E., P.E., Instructor, Department of Civil and Environmental Engineering, Colorado State University, Fort Collins, CO. Email: bob.johnson@colostate.edu (corresponding)

Rebecca A. Atadero, Ph.D., P.E., Assistant Professor, Department of Civil and Environmental Engineering, Colorado State University, Fort Collins, CO. Email: ratadero@engr.colostate.edu

Paper No. 2015-10R

Fig. 1. Bridge over Box Elder Creek, 2005 (reprinted courtesy of AISC).

Fig. 2. Bridge over Box Elder Creek, 2015.

longitudinal reinforcing (the SMC reinforcing) placed over the supports and extended partially or fully into the spans for development (Figure 4). The concrete slab is then placed and allowed to cure and develop bond with the reinforcing steel; at this time, the camber should be nearly equalized. Once the slab has attained design strength, the additional top reinforcing placed over the supports will enable the composite section to resist negative moments and, in effect, become continuous for live and superimposed dead loads. The ability to resist negative moments, along with the combined positive moment strength of the composite section, create a nearly continuous girder with significant strength (Figure 5).

The behavior of SMC bridges better balances the interior positive and continuous end negative moments than fully continuous girder bridges. In addition, SMC bridges actually have smaller negative moments over the supports than fully continuous girder bridges; negative moments control the design of fully continuous bridges as they are primarily resisted by the steel girder, with a small portion possibly resisted by longitudinal slab shrinkage reinforcing. The positive moments in SMC bridges are larger than those in

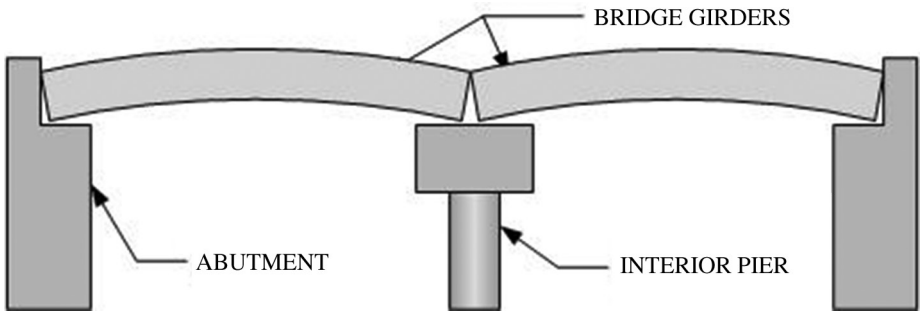

Fig. 3. Girders placed on supports.

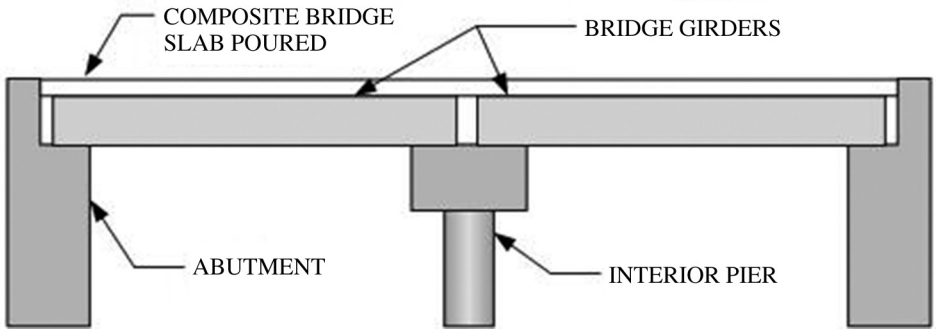

Fig. 4. Bridge deck slab cast on girders.

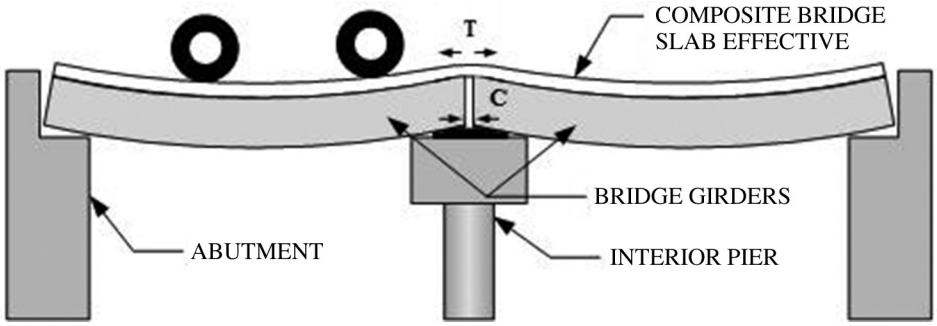

Fig. 5. Slab strength and continuity attained.

the fully continuous bridges; however, the total moment range (the sum of the absolute value of the negative moment and positive moment for a particular span) is less for SMC bridges. Figure 6 shows the combination of dead and live loads on a sample SMC bridge. The sample bridge consists of two equal 140-ft spans; the superstructure is constructed of a 10-in.-thick composite slab supported by 54-in.-deep plate girders spaced at 10 ft on center. For the first stage, when the girder is carrying the slab noncompositely, the maximum factored dead load positive moment is 4,835 kip-ft. In the SMC condition, the maximum factored positive moment is 7,450 kip-ft, while the maximum factored negative moment is 5,860 kip-ft (factored dead and live load moment range = 13,310 kip-ft). Figure 7 compares the combined moment diagrams of the sample SMC bridge to the moment diagram of a fully continuous bridge, which has maximum factored positive and negative moments of 5,585 kip-ft and –11,214 kip-ft, respectively (factored dead and live load moment range = 16,800 kip-ft). While the SMC bridge has a higher positive moment, this moment will be taken by the girder and slab in composite action; the significant advantage is the difference in the maximum negative moments. In the SMC bridge, the post-composite action negative moment is resisted by the girder in composite action with the top-reinforcing steel, whereas in the fully continuous bridge, the negative moment must be resisted by the steel girder section and only slab shrinkage reinforcing, which provides considerably less area of steel than reinforcing designed for SMC behavior. If negative moment redistribution were considered for the fully continuous bridge in accordance with AASHTO article B6.3.3, the maximum reduction to the negative moment would be 20%. The reduced fully continuous moment would be 8,971 k-ft, which is still 68% greater than the SMC negative moment.

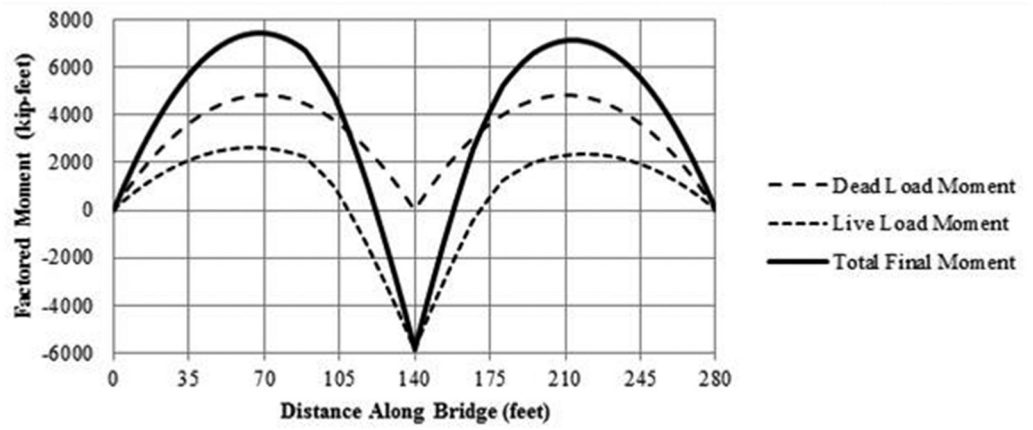

Fig. 6. Simple-made-continuous two-span bridge behavior.

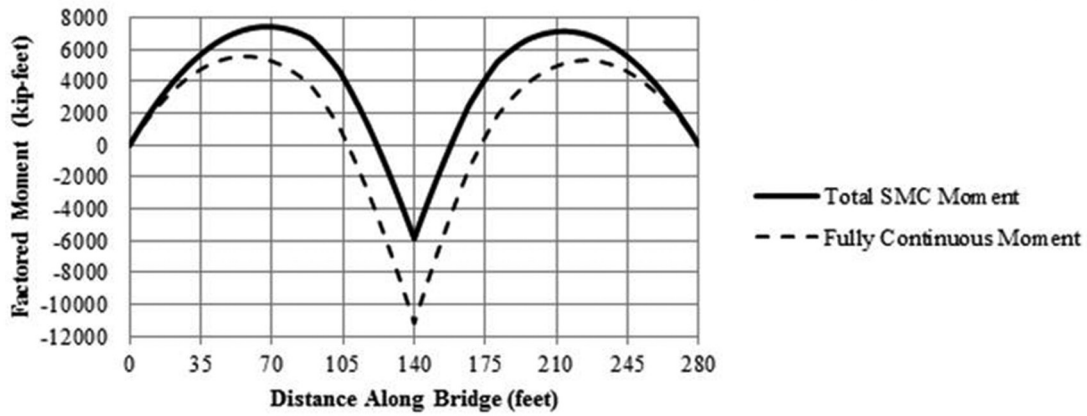

Fig. 7. Comparison of factored moments between two-span fully continuous and SMC bridge girders.

BASIC CONNECTION BEHAVIOR

The SMC connection investigated consists of four basic load transfer elements (Figure 8):

1. SMC top-reinforcing steel.
2. Girder bottom flange.
3. Welds to bearing plate.
4. Bearing/transfer plate.

The factored moment at the continuous end of the girder is resisted by a couple between the girder bottom flange and the SMC reinforcing steel in the slab. At the end of the girder, the compression in the bottom flange is transferred by the welds to the bearing/transfer plate. The bearing/transfer plate then transfers the load from one girder end to the adjacent girder end.

While this connection detail appears simple and straightforward, there are several potential points of weakness in the design. The compression component of the moment must be resisted by shear in fillet welds in order to transfer to the adjacent girder. Failure of these welds would result in nonductile behavior; also, basic hand analysis of the force components in the connection indicated that the weld on the Box Elder Creek bridge in particular may be too small. In addition, the weld in the position used raises fatigue concerns about the connection. While the girder bottom flange and the bearing plate are transferring the load in compression, the weld is transferring load in shear. Based upon the uniqueness of this connection and concerns regarding the weld capacity, this connection was chosen for further study, including finite element analysis (FEA) and a physical test of the connection in the lab.

PRELIMINARY FINITE ELEMENT ANALYSIS

Finite element analysis (FEA) of the connection was performed using Abaqus finite element software. Various material models for the concrete, structural steel, reinforcing steel and welds were investigated until models with behavior that agreed within roughly 10% or less with approximate hand calculation results on a simplified bridge structure were found. The structural steel and reinforcing steel were modeled as a linear elastic material up to yield and then modeled as nonlinear up to their corresponding ultimate strengths. A concrete damage model presented by Carreira and Chu (1985) was used for the concrete slab. Following the material model selection, a sensitivity analysis was performed to determine element types to optimize both the speed of analysis and correctness of results. On the basis of the sensitivity

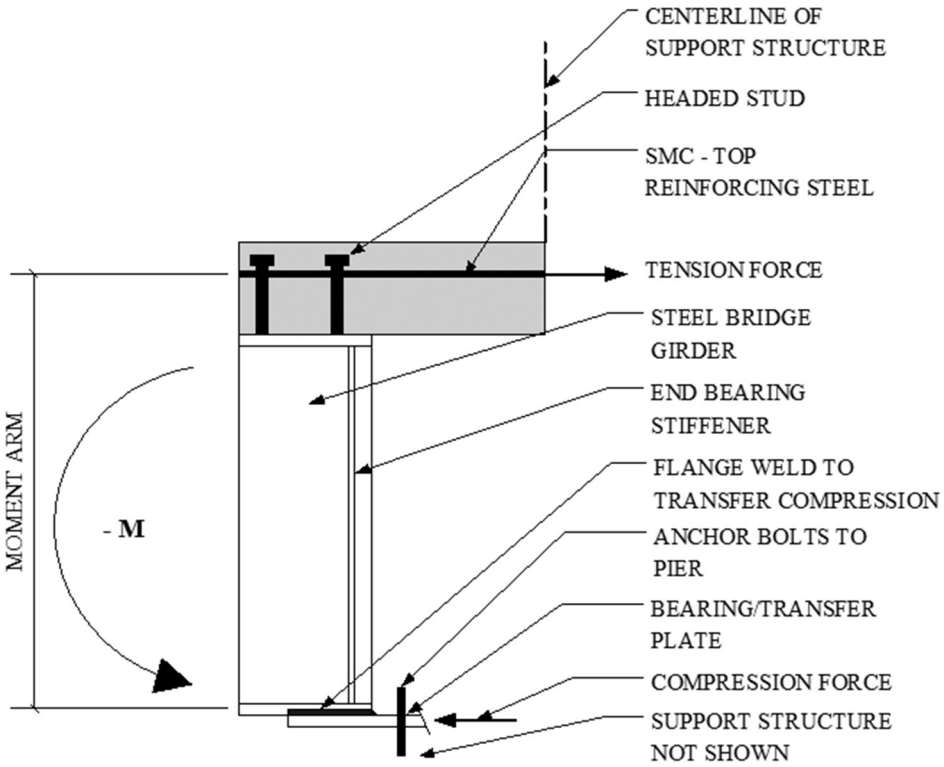

Fig. 8. Girder SMC behavior.

analysis, the element types and meshing of the full connection model were modified to take advantage of the results. The concrete slab, structural steel shapes and reinforcing steel were all modeled using linear brick elements because the use of higher-order elements provided virtually no additional accuracy in results; shear studs were modeled as beam elements. The slab connection to the studs was modeled as a tie, and the reinforcing steel was modeled as embedded in the slab.

Based on comparison with the physical test, the final FEA results provided close results for internal forces in the SMC reinforcing, girder flanges, welds and bearing/transfer plate. Of particular interest, it was noted in the FEA model that there was a reduction of the moment at the centerline of the connection due to the actual location of the reaction force not being at the center of the support, but rather at various locations under the girder end depending upon load. This effect is shown in Figure 9, which presents results of the FEA showing the moment diagram at an applied load of 98 kips, which in theory would result in a centerline moment of −1176 kip-ft instead of the actual centerline moment of 970 kip-ft. It is evident that the moment reduces once the girder bearing/transfer plate becomes involved; there is also a slight reduction in the negative moment up to the center of the plate (0 on the X-axis) and then the behavior mirrors for the adjacent girder. This effect was also observed in the physical test, although with fewer data points. Also noted in the FEA results was that the longitudinal axial stresses at isolated locations in the vicinity of the center of the bearing/transfer plate (Figure 10) were in excess of yield stress by nearly 40%. Figure 10 also shows the location of the girder bearings, which are denoted by dashed black lines, and the locations of the welds, which are denoted by solid black lines.

The deflection at the end of the slab predicted by the FEA model was found to be about 50% of that recorded during the physical test. It appears that the difference in behavior was most likely due to the concrete material model used. Modifications to the FEA model—including varying the concrete modulus of elasticity in the slab to simulate the decreased effect of the stiffness of the concrete at the extremities of the model and at areas of cracking in the top of the slab—were considered after the physical test results were available. These modifications were able to improve the correlation between the FEA and physical test deflections. These modifications were based on physical understanding of what the concrete should be experiencing during the test, but further study is needed to provide modeling guidance that can improve a priori predictions when no test data are available for calibration.

EXPERIMENTAL TESTING OF FULL-SCALE CONNECTION

A physical test of the full-scale connection was conducted in the structures lab at Colorado State University (Johnson, 2015). The test specimen consisted of a center connection with two 15-ft cantilevered spans loaded with hydraulic actuators at the cantilever ends, 12 ft from the center of the connection (Figure 11). The connection was constructed as

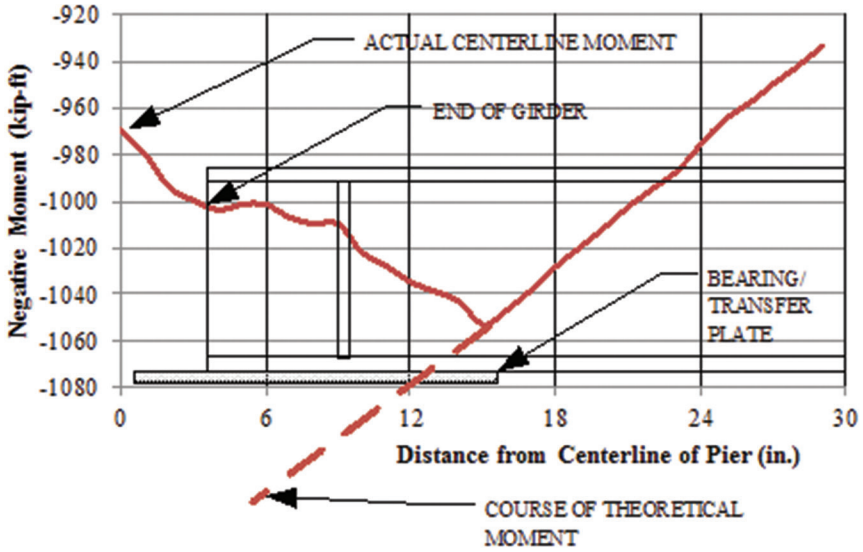

Fig. 9. Girder moment behavior over support.

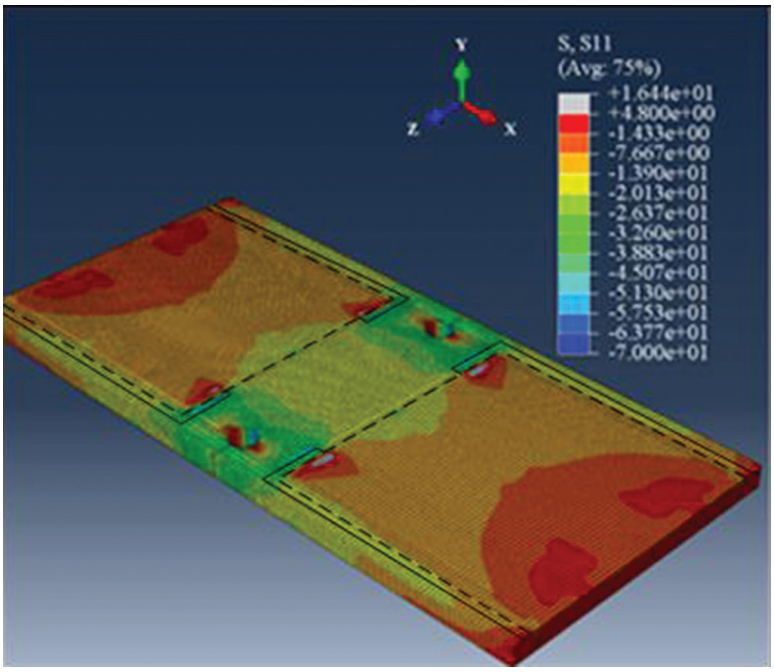

Fig. 10. Longitudinal axial stress in bearing plate (the extent of the girder bearings are indicated by the dashed lines, and the extent of the welds are indicated by the solid black lines).

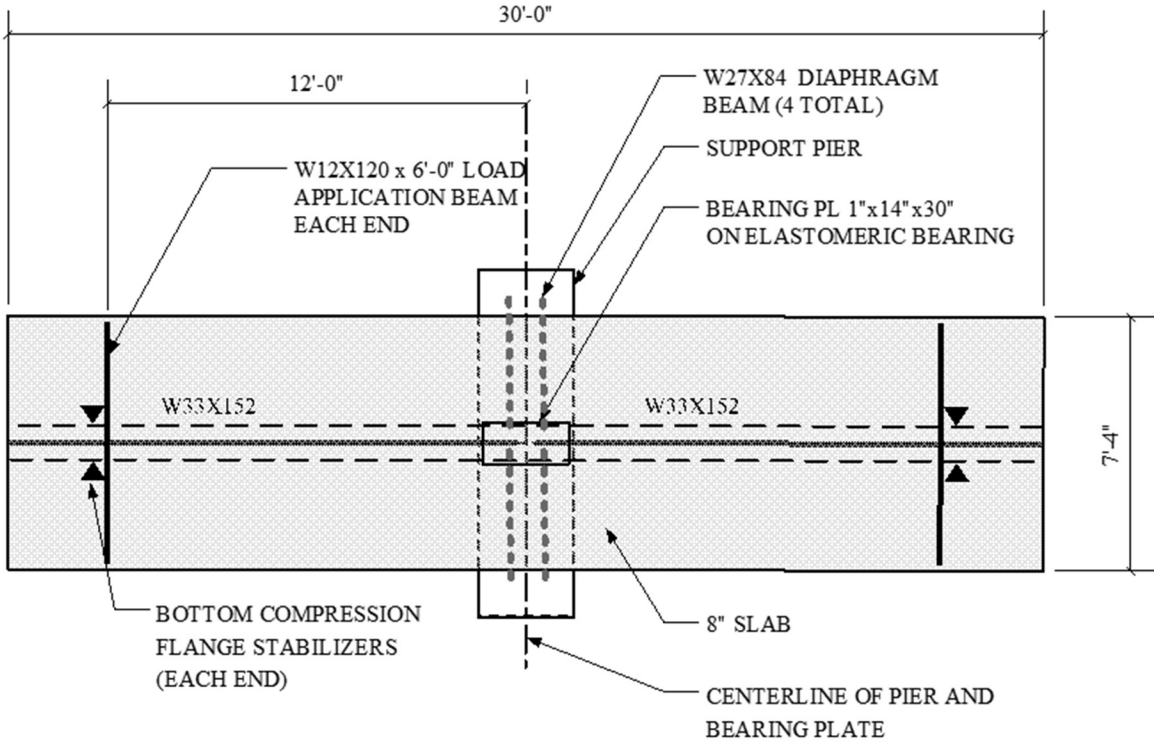

Fig. 11. Physical test specimen plan layout.

indicated in the original drawings, except for the addition of a safety device installed between the ends of the girder bottom flanges (Figures 12 and 13) to be activated in the event the welds failed as anticipated. The plate was initially installed with a gap of 1/16 in. at each side so that it did not engage prior to the anticipated failure of the fillet weld of the girder end to the bearing/transfer plate. Also, the size of the welds on one of the girder end connections was increased to ensure that both would not fail simultaneously. The final test configuration is shown in Figure 14; the center SMC connection showing the steel-diaphragm beam and the safety device is shown in Figure 15. The diaphragm beam was used in the test specimen to laterally stabilize the girder, which is its key function in the actual bridge.

During the test, the connection was loaded by displacement control at a rate of 0.02 in./min. The test specimen performed well until an actuator load of 80 kips was applied at each end, resulting in an approximate centerline moment of 960 kip-ft. At the 80-kip load point the specimen emitted a loud bang as the girder bottom flanges made sudden contact with the safety device, which then became engaged (Figure 12). The testing was stopped and the actuators withdrawn from the test specimen. Upon visual examination of the welds and review of the strain data, no failure of the welds was evident.

Further analysis was then performed on the connection design, and it was determined that the bearing/transfer plate had yielded due to a combination of bending (both from rotation of the attached girder and the eccentric loading of the weld), axial load and deformation of the elastomeric bearing; this behavior is diagrammed in Figure 16. The following day, the cantilever ends of the test specimen were shored up, and the safety device was removed and machined down 1/8 in. in order to allow a slightly larger gap between it and the girders. The safety device was then reinstalled and the test recommenced.

During the recommenced test, at an applied load of 120 kips, which resulted in an approximate centerline moment of 1,440 kip-ft, there was another loud bang, again due to the safety device (Figure 12) becoming activated. The loading was halted and the actuators unloaded. The welds matching the actual construction (north connection) were examined and found to be cracked along the sides and end of the girder. Based on original hand calculations for the strength of the weld and the behavior of the connection, the estimated ultimate moment for the welds was 1433 kip-ft. Testing thus confirmed that the welds were undersized.

Following the examination of the connection and verifying that the safety device was properly seated, the test was restarted again. Due to limitations of the actuators and the load frame used for the test, the maximum load that could be applied at each girder end was 200 kips, and this full load was successfully applied to the connection, producing in a theoretical centerline moment of 2400 kip-ft without incident. The 2400-kip-ft moment is well in excess of the maximum ultimate design moment of 1783 kip-ft.

Strain gages positioned on the SMC reinforcing, the bearing/transfer plate and the safety device provided additional information about the behavior of the connection. Figure 17 shows the axial force in the top SMC bars and also the top SMC bars in combination with the top temperature bars at the center of the connection; this diagram gives a clear picture of the shear lag behavior in the slab. For comparison, the shear lag from the FEA is also shown, which is very similar in shape and varies by a maximum of approximately 10%. Reviewing the shear lag behavior of the connection (Figure 17), it is apparent that the bars immediately adjacent to the bar directly over the girder take a disproportionate share of the SMC tension component. In the case investigated, the bars immediately adjacent to the center bar each resisted 8% of the total SMC tension. Research performed at the University of Nebraska (Niroumand, 2009) indicated that for

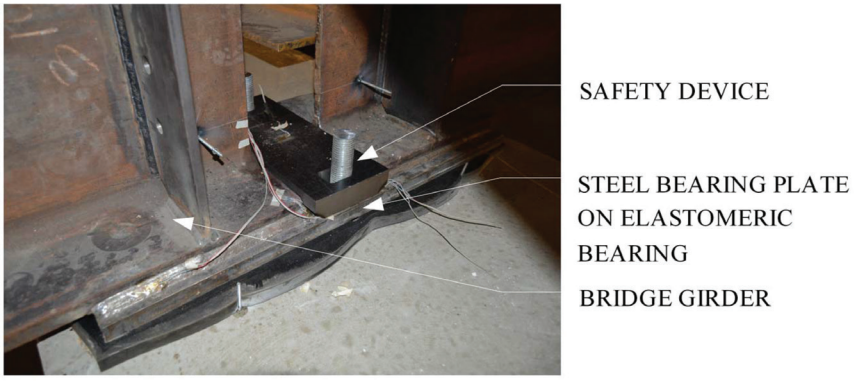

Fig. 12. Safety device at end of physical test.

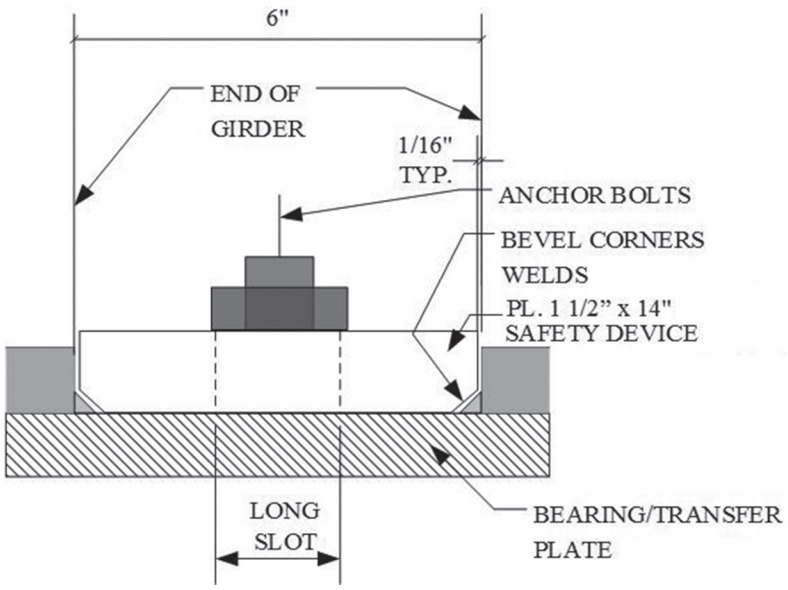

Fig. 13. Construction detail of safety device.

Fig. 14. Physical test specimen.

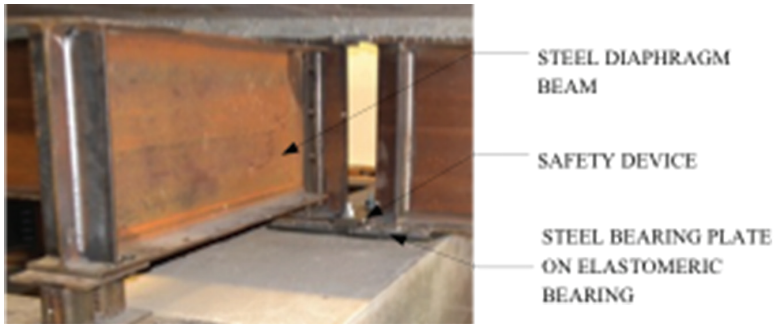

Fig. 15. Detail at steel diaphragm.

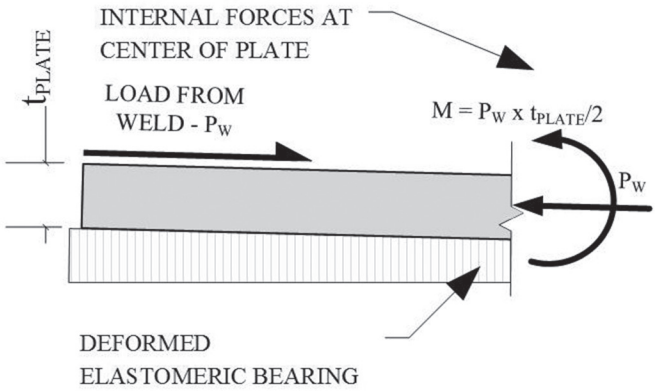

Fig. 16. Effects of load eccentricity at center of bearing plate.

Table 1. Comparison of Theoretical and Actual Moments at Centerline of Physical Test Specimen			
Event	Theoretical Moment at Center of Support, kip-ft	Actual Moment at Center of Support, kip-ft	Center of Actual Bearing from Center of Bearing Plate, in.
End of day 1 test, load = 135 kips	1620	1490	12
Activation of safety device, day 2 test	1440	1370	10.5
End of day 2 test, load = 196.5 kips	2360	2230	8

SMC bridges, loaded such that the top reinforcing begins to yield near the center (as is the case herein), and upon the application of additional load, the adjacent bars would begin to take more load and the behavior would continue to propagate until the last bars in the effective width had yielded. While this behavior is acceptable in an overload condition, having the center bars and adjacent bars possibly going plastic under normal service conditions would be unacceptable due to excessive slab cracking and permanent elongation in the SMC reinforcing. Thus, in order to prevent yielding of the most highly stressed SMC bars, it is recommended that additional bars be placed adjacent to the as-designed SMC reinforcing. The best way to achieve this is by placing the longitudinal top shrinkage reinforcing at the same spacing and adjacent to the SMC reinforcing and using a minimum of #5 bars. As it so happens, all of the SMC bridges reviewed for this study spaced the top shrinkage reinforcing bars at the same spacing as the SMC reinforcing, which was most likely for ease of placement and to avoid confusion. Further study of the shear lag phenomenon is recommended to evaluate the behavior of the SMC reinforcing bars acting with the shrinkage reinforcing to verify that they have the capability to prevent the center SMC bars from yielding.

Comparison of the physical test results to hand calculations of the moments indicated that the actual centerline moment was less than that predicted by hand calculation on an ideal cantilever. Figure 18 and Table 1 show the theoretical centerline moment as that calculated using a point support of the SMC girder, while in actuality, the girder begins to be supported and thus relieved of load at the face of the bearing/transfer plate; this was also the case in the finite element analysis as shown in Figure 9. The actual moment is the moment at the center of the support based on the actual support condition. The actual moment values are as shown in Table 1 and were determined by evaluating strains in the SMC reinforcing steel, the bearing/transfer plate and the safety device; their moment arms were then used to the current neutral axis—i.e., assuming the web carries no moment. Table 1 also lists the distance from the center of actual bearing to the center of the bearing/transfer plate. This phenomenon again is due to the reaction being under the beam bearing and, in actuality, much closer to the position of the beam bearing stiffener; this behavior would also occur in the actual bridge, a continuous-for-live-load structure. This

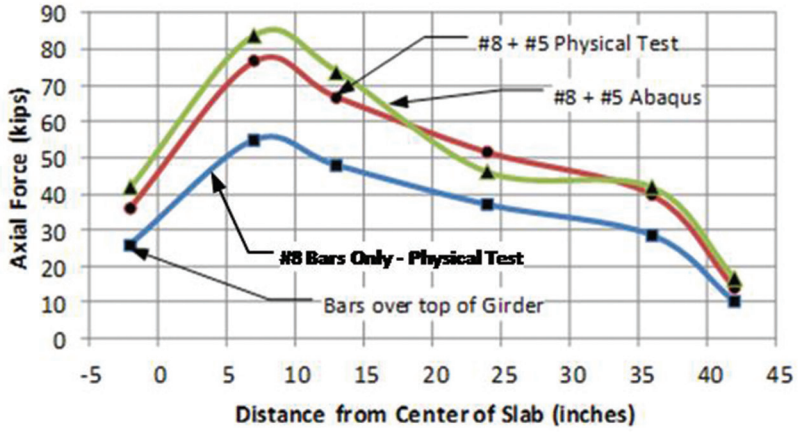

Fig. 17. Axial force in top slab bars at center of connection—physical test vs. Abaqus.

means that designing the connection for the full theoretical centerline moment would be somewhat conservative.

RECOMMENDED IMPROVEMENTS TO DESIGN AND DESIGN METHODOLOGY

The scheme investigated has several design flaws, specifically the welds to the bearing/transfer plate and the bearing/transfer plate itself. The welds are undersized and thus inadequate to resist the maximum design loads. In addition, the welds would be subject to a load-induced fatigue category E′, which limits the constant amplitude fatigue threshold to 2.6 ksi, a fatigue range that would be far exceeded during the course of regular service of the bridge. The bearing/transfer plate, which is connected to the girder bottom flange by the aforementioned welds, is unable to resist the combined effects of the axial compression and the moment induced into the plate by the eccentricity of this compression. In order to avoid plate and weld failure and subjecting the welds to fatigue, a direct means of load transfer between the bottom girder flanges would be desirable.

As was described in the testing portion of this article, a safety device (Figure 13) was installed in the event that the welds failed, and during testing, this device successfully transferred the compressive force component of moment when the bearing/transfer plate failed. Due to the satisfactory behavior of this device, it is recommended that a transfer device similar to the safety device be used in new designs, omitting the welds to the bearing plate and any connection of the girders to the base plate. This modification to the connection will be a definite improvement to the scheme investigated, in both strength and economy. A proposed solution is shown in section in Figure 19 and in plan in Figure 20; this detail provides two wedge-shaped plates to allow for field fit-up based on designs used in partial SMC bridges in Tennessee (Talbot, 2005). The girders are laterally supported by anchor bolts through their bottom flanges and cast into the support pier.

The design methodology for the proposed scheme involves three major steps: (1) preliminary steel girder design, (2) design of SMC top-reinforcing steel based on the girder size and (3) verification of the girder size. Design of the steel girders is based on:

1. Their strength and stability to support themselves, formwork, wet concrete and any construction live load as noncomposite, simple beams.
2. Their composite positive moment strength to support the superimposed loads from the SMC behavior along with the locked-in forces from item 1.
3. Additionally, the composite girders must be evaluated to meet all the post-composite strength and serviceability requirements, in particular, deflection. These girders are typically cambered for the dead loads of the girder and the composite slab, so only deflection due to post-composite loads needs to be considered.

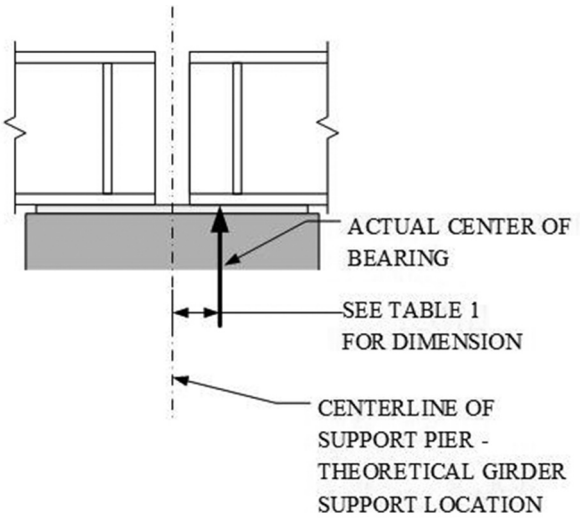

Fig. 18. Theoretical vs. actual center of girder bearing.

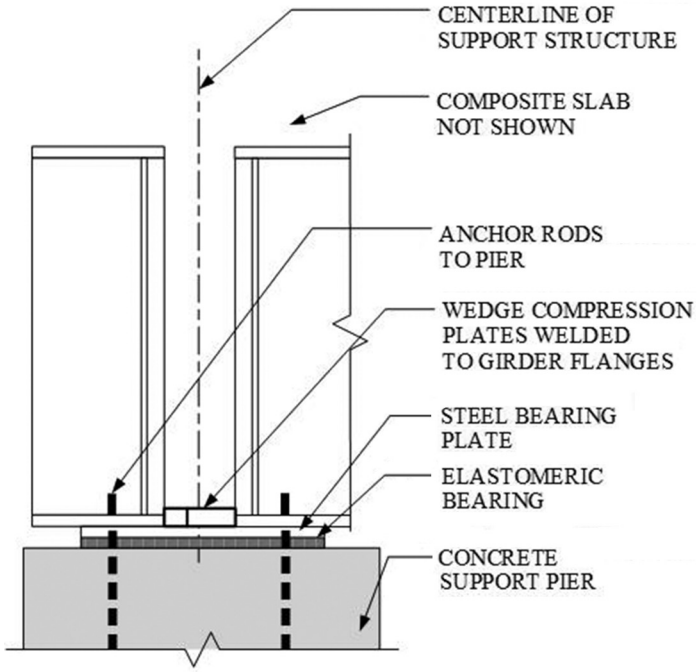

Fig. 19. Recommended revised bearing plate section.

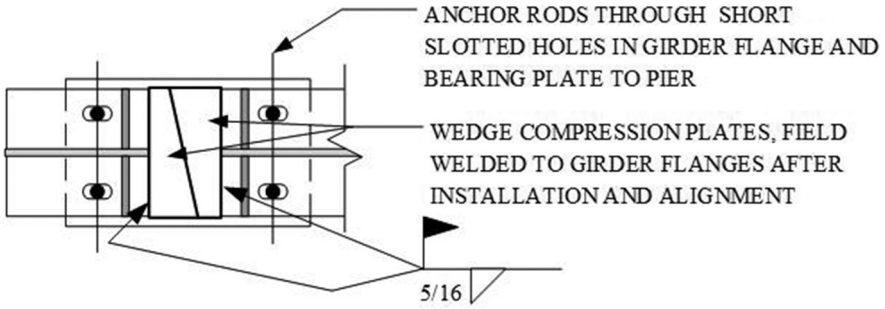

Fig. 20. Recommended revised base plate plan.

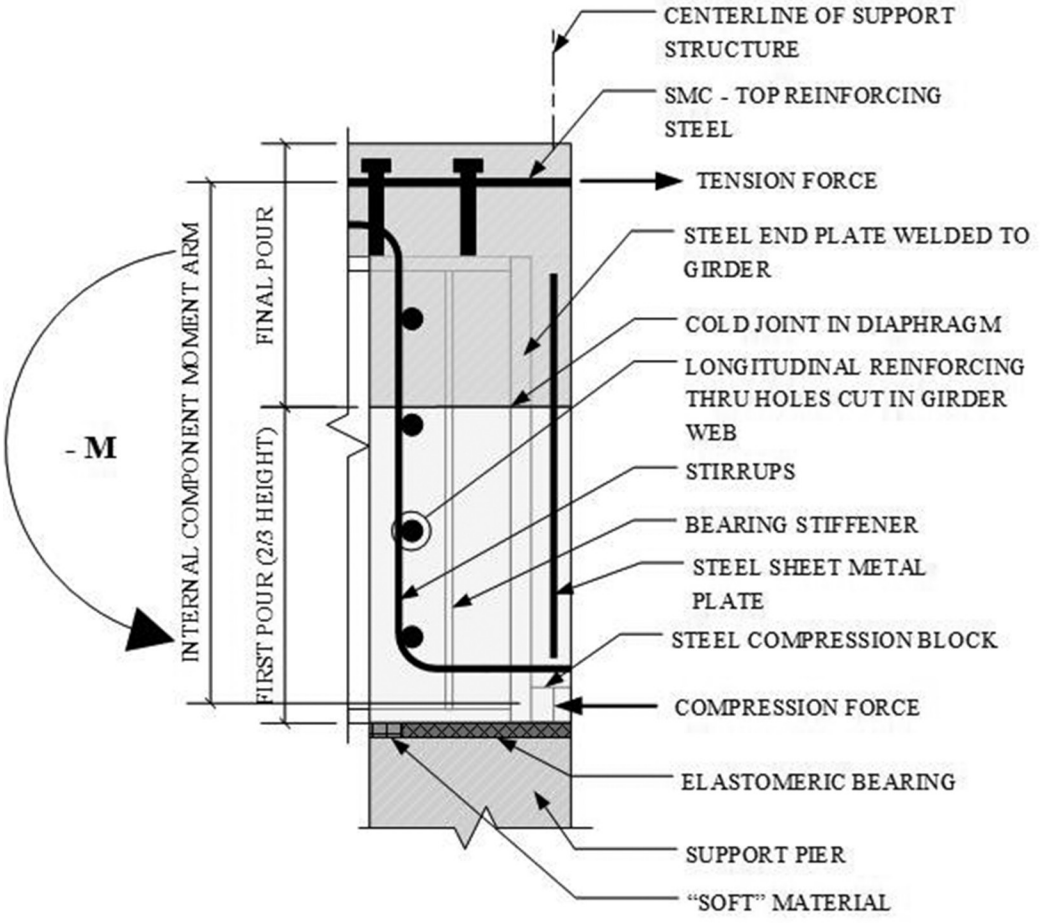

Fig. 21. Details of SMC connection (Azizinamini, 2014b).

After the girders are sized, design of the remaining connection elements is relatively straightforward, and the overall behavior is similar to that developed by researchers studying SMC connections with concrete diaphragms (Azizinamini, 2005, 2014b). The current concrete-diaphragm scheme proposed and developed by these researchers and currently in use is shown in Figure 21; this detail basically resists the SMC moment by a couple between the SMC top-reinforcing and steel-compression blocks between the bottom flanges and portions of the webs of the girders. For the steel-diaphragm scheme proposed herein, there are two important differences: The first is not encasing the connection in a concrete diaphragm, but rather leaving the connection exposed and using steel diaphragms. The second is that the compression component is transferred only between the girder bottom flanges using longitudinally adjustable wedge compression transfer plates because, with this SMC scheme, only the bottom flange is considered to resist the compression component of the SMC behavior. The wedge plates should be ⅜ in. or greater in thickness than the bottom flanges in order to provide sufficient depth for the weld to the girder flange. By considering only the bottom flange in compression, the internal moment arm is larger and thus will require less total resultant force in the tension and compression components for the same moment capacity (Figure 22); this is not to say the stresses will be lower, only the resultant couple forces. After the girder size has been established, the moment arm between the girder bottom flange and the SMC top-reinforcing steel is easily determined as it is a function of all known values and an assumed SMC reinforcing bar diameter. For 50-ksi girder steel and 60-ksi reinforcing steel, the area of the reinforcing steel can be easily determined by directly equating the total area of SMC reinforcing steel required to the area of the girder bottom flange without regard to the differences in yield strength or resistance factors, which will add a very slight conservatism to the design.

Once the reinforcing steel area is known and the resultant moment arm determined, the final check of the girder is to verify that the moment capacity developed is adequate for the design negative moment due to the SMC behavior. This is accomplished by multiplying the girder flange area by the yield strength of the flange (resistance factor, $\phi = 1.0$) and then by the moment arm determined. The resultant internal moment strength from the previous calculation should be compared with the actual factored design negative moment in the bridge; if the applied factored moment is less than the strength, then the connection is adequate. Otherwise, the girder size should be increased to the next available shape in

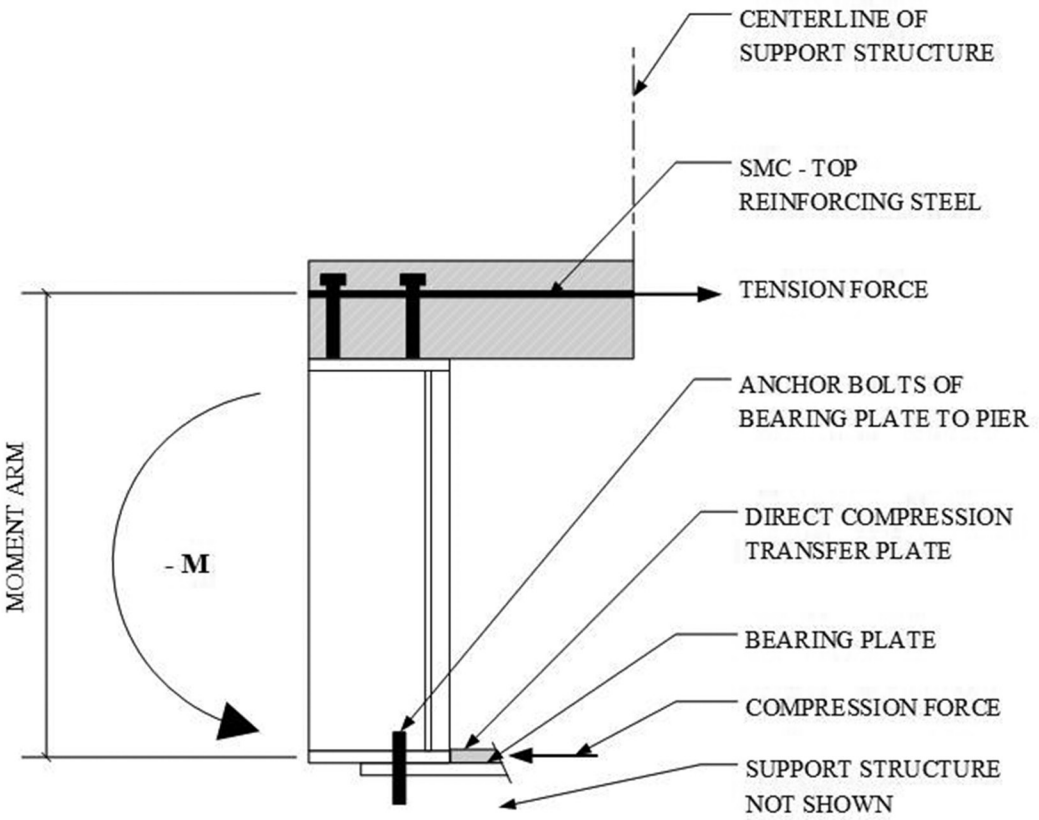

Fig. 22. Final proposed support detail.

the depth range and the second and third steps repeated. If the next girder is a deeper depth range, it would be prudent to reanalyze the bridge because there could be load distribution consequences based on the increased depth and corresponding increase in stiffness. It is important to note that this is a somewhat simplistic design methodology for a connection with a complex behavior and not fully continuous behavior. Full continuity of the girder would require continuity of the webs; however, it is apparent that the stiffness of the webs relative to moment resistance is a small fraction (≤20% based on comparison of sample Z_x's of various shapes) of that of the flanges and SMC reinforcing. Based on the additional conservatism of using the theoretical factored centerline moments versus actual factored moments (Table 1), a typical continuous girder analysis for superimposed dead and live loads would be reasonable for design. It should be noted that no other SMC connection or partial SMC connection reviewed has a positive full-height connection between girder webs.

The design procedure for the SMC connection components based upon a selected girder size is outlined here:

1. Design of SMC reinforcing. Equate the area of SMC reinforcing to the area of the bottom flange:

   $A_r = A_f = b_f t_f$

   where

   A_r = required area of SMC reinforcing steel, in.^{2}
   A_f = area of girder bottom flange, in.^{2}
   b_f = width of bottom flange, in.
   t_f = thickness of bottom flange, in.

   The recommended minimum bar size is #8; smaller bars would require a significantly greater number (over 30%) of bars be placed.

2. Determine the moment arm of the couple between the girder bottom flange and the SMC reinforcing based on girder and slab geometry:

   $$d_m = d_h + t_s - cl - D_t - \frac{D_{SMC}}{2} + d_G - \frac{t_f}{2}$$

   where

   d_h = depth of haunch, in.
   t_s = tickness of slab, in.
   cl = reinforcing clear distance, in.
   D_t = main (lateral) top reinforcing bar diameter, in,
   D_{SMC} = SMC (longitudinal) reinforcing bar diameter, in.
   d_G = depth of firder flange, in.
   t_f = tickness of girder flange, in.

3. Verify the moment capacity of the section designed using the area and yield stress of the girder flange:

   $\phi M_n = A_f d_m F_{yG}$

   where

   ϕ = 1.0 for the steel girder
   M_n = nominal moment capacity, kip-in.
   A_f = area of the bottom flange, in.^{2}
   d_m = moment arm between SMC reinforcing and center of bottom flange, in.
   F_{yG} = Yield stress of firder flange, ksi

4. Size the compression transfer wedge plates based upon girder bottom flange dimensions:

   $w_{tp} = b_f + ½$
   $t_{tp} = t_f + ⅜$

   where

   w_{tp} = minimum width of transfer plate, in.
   b_f = width of girder bottom flange, in.
   t_{tp} = minimum thickness of transfer plate, in.
   t_f = thickness of girder bottom flange, in.

A design example is presented next for a bridge with 80-ft girder spans, a 9-in.-thick slab, 9-ft girder spacing and #9 SMC reinforcing bars. From a strength and serviceability analysis of the composite section for positive moments, a W33×169 was selected. The SMC moment is –2248 kip-ft.

b_f = 11.5 in.
t_f = 1.22 in.
d = 33.8 in.
A_f = (1.22 in.)(11.5 in.) = 14.03 in.^{2}
d_h = 3.00 in.
t_s = 9.00 in.
cl = 2.50 in.
D_t = 0.625 in. (#5 bar)
D_{SMC} = 1.125 in. (#9 bar)
d_g = 33.8 in.
t_f = 1.22 in.

$$d_m = 3.00 \text{ in.} + 9.00 \text{ in.} - 2.50 \text{ in.} - 0.625 \text{ in.} - \frac{1.125 \text{ in.}}{2} + 33.8 \text{ in.} - \frac{1.22}{2} \text{ in.} = 41.5 \text{ in.}$$

$$\phi M_n = \frac{14.03 \text{ in.}(41.5\text{in.})(50 \text{ ksi})}{12 \text{ in./ft.}} = 2{,}426 \text{ kip-ft}$$

> 2,248 kip-ft **o.k.**

Determine SMC bar quantity and spacing:
A#9 = 1.00 in.^{2}
N = 14.03 in.^{2}/(1 in.^{2}/bar) = (14) #9 bars
Slab width = 9.00 ft = 108 in.
Spacing = 108 in./14 bars = 7.7 in./bar; use #9 at 7½ in,

Compressions transfer plate size:
$t_{tbmin} = t_f + 0.375$ in. = 1.22in. + 0.375 in. = 1.595 in.
$W_{tbmin} = b_f = 11.5$ in. + 1.00 in. = 12.5 in.
Use compression transfer plate: 1⅝ in. × 12½ in.

Table 2. Comparison of SMC to Fully Continuous Moments					
	Location				
Bridge Type	Span 1 Interior, kip-ft	Spans 1 and 2 Support, kip-ft	Span 2 Interior, kip-ft	Spans 2 and 3 Support, kip-ft	Span 3 Interior, kip-ft
SMC	+2460	–1970	+2030	–1640	+2110
Fully continuous	+2170	–2730	+1420	–2180	+1570

Table 3. Material Unit Costs		
Material	Unit Cost	Units
Structural steel	$2500	Ton
Girder splice (Azizinamini A., 2014)	$2000	Each
Epoxy-coated reinforcing steel	$1685	Ton

Table 4. Girder Cost Comparison Fully Continuous Bridge to SMC Bridge per Girder		
Element	Fully Continuous	Simple-Made-Continuous
Girder	$19,360	$14,790
Splice	$2,000	0
SMC reinforcing	$0	$2,580
Total cost	$21,400	$17,400
Cost difference	23.0%	

COMPARISON TO FULLY CONTINUOUS STEEL BRIDGES

SMC construction has been touted as a way to make construction with steel more cost effective (NSBA, 2006). To compare the costs with the steel-diaphragm connection, the State Highway 36 bridge over Box Elder Creek was analyzed for the as-constructed SMC condition and as a fully continuous for all loads condition. The girders spans (77 ft 10 in.), girder spacing (7 ft 4 in.) and slab thickness (8 in.) were the same for both bridges. Maximum positive and negative moments in the first two spans of this six-span bridge are shown in Table 2. As is evident, the negative moments are considerably larger for the fully continuous girder bridge and, thus, would require larger girders than the SMC girder bridge. This is a significant point because it means that the SMC girder bridge would not only be simpler and faster to construct than a conventional fully continuous girder bridge, but it would also be more economical by requiring lighter girders.

The fully continuous girder bridge required to resist the negative moments would be a W40×199, W36×231 or W33×241 girder, depending upon depth restrictions. The SMC girder was a W33×152, and the SMC reinforcing consisted of approximately 14.5 #8 epoxy-coated SMC reinforcing bars full span. The slab bending and shrinkage reinforcing was assumed to be the same for both bridges. Assuming no depth restrictions and selecting the lightest size, W40×199, and using the unit costs shown in Table 3, a cost comparison was performed and is shown in Table 4. For a six-span six girder bridge, the total cost savings is more than $143,000. The cost comparison used data from RS Means *Open Shop Building Construction Cost Data* (Waier, 2003); this particular edition was selected for ease of cost comparisons with other SMC bridge schemes with documented cost information.

COMPARISON TO STEEL BRIDGES USING OTHER SMC CONCEPTS

The most commonly used SMC scheme is one in which the steel bridge girders are encased in concrete diaphragms at the piers; based on all available data, this design appears to have been developed by researchers at the University of Nebraska. The Nebraska researchers based their use of a concrete diaphragm for this scheme on the existing Nebraska Department of Roads standards (NDOR, 2001)

used in the design of precast concrete girder SMC bridges without any other justification (Azizinamini, 2005). The use of the aforementioned scheme led to cracking at the ends of the concrete diaphragms; thus, in subsequent designs, gage metal steel plates were installed into the pier diaphragms during their construction to alleviate the cracking (Azizinamini, 2014b).

The installation of the girder ends into a concrete diaphragm is not only a time-consuming process, but also requires additional construction time. Moreover, there are possible effects on the long-term performance of the connection, specifically:

1. The diaphragm concrete may develop cracks at reentrant corners of the girder.
2. If cracks develop in the diaphragm, this may allow moisture to penetrate into the diaphragm, potentially causing freeze-thaw damage.
3. The girder ends and, particularly, the SMC transfer mechanism are not visible for periodic inspection.

A comparison of diaphragm construction costs was made between the two methods as the diaphragm construction for either scheme would not vary significantly (<5%) between different bridge girder spans as shown in Table 5. The bridges used for comparison are the bridge carrying Sprague Avenue over I-680 in Omaha, Nebraska (Sprague Street Bridge), and the bridge carrying Colorado State Highway 36 over Box Elder Creek (Box Elder Creek Bridge). For better comparison, the diaphragm beam size for the S.H. 36 bridge was increased in size to better correspond with the depth of the girders used on the Sprague Street bridge. As may be seen, the cost of a steel diaphragm is approximately 5% more than of that of a cast-in-place diaphragm, which, in comparison to the total cost of the bridge, is negligible because for the bridges considered in the comparison, the diaphragms occur 77 ft on center or greater. Also, a construction man-hour comparison is made between the two types of diaphragms and is shown in Table 6. As is evident, the number of man-hours per foot of diaphragm construction for the steel-diaphragm bridge is only 6% of that for the concrete-diaphragm bridge, which is notable because this would affect the total construction time involved to construct the bridge. Also, for the concrete-diaphragm bridge, it was recommended that the concrete diaphragm be allowed to cure for 7 days (Azizinamini, 2014b) prior to placement of the remaining one-third of the diaphragm and the bridge slab; this would not be the case with the scheme using steel diaphragms. Using steel diaphragms attached to full-height stiffeners will completely brace the top flange, whereas in the concrete-diaphragm scheme, the top third of the girder is effectively free to buckle until the concrete has attained some strength.

CONCLUSIONS

This article presented and discussed simple-made-continuous (SMC) bridges and, in particular, a scheme that uses steel diaphragms in lieu of concrete diaphragms for lateral and torsional restraint over the supporting piers. Based on physical testing, the original detail considered was found to have weaknesses in its compression load transfer mechanism; these weaknesses were addressed by using direct compression transfer plates. The SMC connection using steel diaphragms was shown to be quicker to construct than other current SMC schemes and more economical and faster to construct than fully continuous girder bridges. Also presented herein was a proposed design methodology based on research performed at Colorado State University.

The testing program described herein had several limitations. The maximum applied load at each end was limited to 200 kips by the capabilities of the lab equipment, and thus, while several elements were taken beyond their capacity, more information would have been gained had the equipment been capable of loading the structure to yield the SMC reinforcing steel. Additionally, the application of more load may also provide additional information on the slab behavior. As noted earlier, further study of the shear lag phenomenon is recommended to evaluate the behavior of the SMC reinforcing bars acting with the shrinkage reinforcing to verify that they have the capability to prevent the center SMC bars from yielding. Also, while an SMC connection using wedge plates for direct transfer of the compression force is in service in Tennessee, wedge plates were not included in this test program. For these reasons, further study/testing encompassing the final connection configuration presented herein is recommended to provide further validation of the proposed design equations.

The research described in this article provides preliminary evidence that a steel SMC connection based on steel diaphragms may be a competitive alternative to a steel SMC bridge with concrete diaphragms. Local labor, material, scheduling concerns and service conditions may contribute to making one alternative more attractive than the other. It is important that designers are aware of this potentially advantageous alternative.

REFERENCES

Azizinamini, A. (2005), *Development of a Steel Bridge System-Simple for Dead Load and Continuous for Live Load, Volumes 1 and 2,* University of Nebraska, Lincoln, NE.

Azizinamini, A. (2014a), "Simple for Dead Load-Continuous for Live Load Steel Bridge Systems," *Engineering Journal*, AISC, Vol. 51, No. 2, 2nd Quarter, pp. 59–70.

Table 5. Cost Comparison—Concrete vs. Steel Diaphragm						
Bridge	**Sprague over I-680**			**S.H. 36 over Box Elder Creek**		
Element	**Quantity**	**Unit Cost**	**Total Cost**	**Quantity**	**Unit Cost**	**Total Cost**
Formwork	69 SFCA	$7.05	$486			
Epoxy-coated reinforcing steel	0.09 ton	$2545	$229			
Cast-in-place concrete	3.5 CY	$116	$371			
Sheet steel plate	1.75 cwt	$52.5	$92			
End plates and welding	2 each	$202	$404			
W27×84 diaphragms				14.67 ft.	$70.6/ft.	$1036
Girder weld to sole plate	3 LF	$12.75/LF	$38	5 LF	$12.75/LF	$64
Total			$1620			$1100
Diaphragm length	10.33 ft			7.33 ft		
Cost/foot	$157			$150		

Table 6. Construction Man-Hour Comparison						
Bridge	**Sprague over I-680**			**S.H. 36 over Box Elder Creek**		
Element	**Quantity**	**Man-Hours**	**Total Hours**	**Quantity**	**Man-Hours**	**Total Hours**
Formwork	69 SFCA	0.163/SFCA	11.25			
Reinforcing steel placement	0.08 ton	16/ton	1.28			
Cast-in-place concrete	3.19 CY	1.067/CY	3.4			
Sheet steel plate	1	2	2			
W27×84 diaphragms				14.67 ft	0.06/ft	0.9
Total			17.9			0.9
Diaphragm length	10.33 ft			7.33 ft		
Hours/foot	1.73			0.123		

Azizinamini, A. (2014b), *Design Guide for Bridges for Service Life,* Transportation Research Board, Washington, DC.

Carreira, D.A. and Chu, K.-H. (1985), "Stress-Strain Relationship for Plain Concrete in Compression," *ACI Structural Journal*, ACI, Vol. 82, No. 6, pp. 797–804.

Farimani, R.S. (2014), Numererical Analysis and Design Provision Development for the Simple for Dead Load-Continuous for Live Load Steel Bridge System, *Engineering Journal*, AISC, pp. 109–126.

Johnson, R.I. (2015), *Simple Made Continuous Bridges with Steel Diaphragms: Tension and Compression Transfer Mechanisms,* Colorado State University, Fort Collins, CO.

NDOR (2001), *Bridge Office Policies and Procedures (BOPP) Manual 200,* NDOR, Lincoln, NE.

Niroumand, S.J. (2009), *Resistance Mechanism of Simple-Made-Continuous Connections in Skew and Non-Skew Steel Girder Bridges Using Conventional and Accelerated Types of Construction,* University of Nebraska, Lincoln, NE.

NSBA (2006), "Steel Bridge Uses Simple-Span-Made-Continuous Construction," *Modern Steel Construction*, September, pp. 18–21.

Talbot, J. (2005), "Simple Made Continuous," *NSBA Steel Bridge News*, October, pp. 1–5.

Waier, P.R. (2003), *Open Shop Building Construction Cost Data,* R S Means, Kingston, MA.